Learning the dynamics of nonlinear systems with regional stability guarantees through linear matrix inequality constraints ⋆

Daniel Frank * **Fahim Shakib** ** **Steffen Staab** *,***

* *Institute for Artificial Intelligence, University of Stuttgart, Germany (e-mail: {daniel.frank, steffen.staab}@ki.uni-stuttgart.de*
** *Department of Mechanical Engineering, Eindhoven University of Technology, Eindhoven, The Netherlands (e-mail: m.f.shakib@tue.nl)*
*** *Electronics and Computer Science, University of Southampton, United Kingdom of Great Britain and Northern Ireland*

Abstract: This paper presents a method that learns a regionally stable recurrent neural network model from a set of input-output data generated by an unknown dynamical system. Relying on *generalized sector* conditions on the deadzone activation function, we first derive sufficient conditions that guarantee forward invariance on a compact set of the state space for any inputs from a given set. Such regional properties lead to less conservative conditions compared to variants that offer a global form of stability, and are in line with the system data that is only observed regionally. Our learning method derives conditions for regional stability using a barrier function approach, leading to models equipped with a certificate of regional stability in a subset of the state space and for a given input set. We illustrate our theoretical result with a numerical example and compare it to methods that impose a global form of stability, which fail to identify the system, and with a method that imposes no stability constraints at all, which does not guarantee a stable behavior within any state or input set.

Keywords: Nonlinear system identification, Machine and deep learning for system identification, Linear matrix inequalities, Barrier functions, Recurrent neural networks.

1. INTRODUCTION

System identification finds a dynamic model from input and output data by minimizing some loss function, e.g., the mean-squared-error (MSE) between predicted outputs and the outputs in the dataset (Ljung, 1999). Recurrent neural networks (RNNs) are particularly well-suited for learning complex nonlinear dynamics RNNs (Beintema et al., 2023; Mohajerin and Waslander, 2019; Bonassi et al., 2022; Revay et al., 2020). Although accurate on the training data, RNNs can fail to generalize to unseen test data, even leading to unstable prediction, which is undesired especially in safety-critical applications. Consequently, there is a shift towards learning with *stability guarantees* (Pauli et al., 2021; Revay et al., 2023; Shakib et al., 2022).

Existing methods typically enforce a form of *global* stability. For example, Revay et al. (2020, 2023) and Yin et al. (2021) enforce global contraction, Shakib et al. (2025) enforces global convergence, while Bonassi et al. (2022) reviews methods that enforce a global form of (incremental) input-to-state stability. Enforcing a global form of stability relates to using the *standard* sector condition, see (Khalil, 2002), to bound the effect of the nonlinearity globally.

In practice, enforcing a global notion of stability has two main drawbacks. First, measured system data is only observed in a region of the input and state space, making it impossible to verify the stability properties of the data-generating system globally. Secondly, conditions for global stability are overly conservative. To address these issues, adopting a regional form of stability is beneficial: it allows for preserving the observed stability property more accurately and enlarges the set of learnable models, since regional stability constraints are less restrictive than global ones (Shakib et al., 2023). Despite these benefits, learning nonlinear dynamics with a regional form of stability is an open problem. Notably, the work in Shakib et al. (2023) proposes a kernel-based method that enforces regional convergence, a property ensuring forward invariance of a compact set for a given set of inputs and guaranteeing that all trajectories originating within this set converge to each other exponentially.

In this paper, we propose a learning method that enforces regional stability of the RNN. In particular, we employ *generalized* sector conditions, which introduce a degree of freedom to fit the sector to the deadzone nonlinearity tightly and are well-established in anti-windup control (see Tarbouriech et al. (2006)) as well as in the control design with RNNs (La Bella et al., 2025). Notably, in

⋆ Daniel Frank is funded by Deutsche Forschungsgemeinschaft (DFG, German Research Foundation) under Germany's Excellence Strategy - EXC 2075 - 390740016. We acknowledge the support of the Stuttgart Center for Simulation Science (SimTech).

these related works, the models are autonomous, i.e., there is no external excitation. Therefore, their direct use in the scope of learning system with inputs is infeasible and requires a non-trivial extension. To address this gap, our first contribution is a convex constraint, in the form of linear matrix inequalities (LMIs), on the learnable parameters that ensures forward invariance of a compact set of the state space for a given set of inputs. Furthermore, these conditions provide a regional input-to-state stability bound for all trajectories originating within this set.

The second contribution is a learning framework that enforces the derived regional-stability conditions on the learned RNN. Hereto, we equip the MSE loss with a barrier function to enforce the convex constraints during learning. This approach is scalable to models with a large number of parameters, as no LMIs need to be solved during training. The resulting RNN is regionally stable, with the most suitable compact state space set, i.e., the region, emerging from the training process for a given input set. This learning method requires an initial RNN that already satisfies the convex constraints, for which we present a separate result.

The contribution of our work can be summarized as follows:

- We provide convex constraints for regional stability of RNNs with external inputs.
- We provide a learning framework that enforces the constraints using a barrier function approach.

The theoretical results are supported by a numerical experiment, which demonstrates recovering a regionally stable system from input-output data. We compare our approach with a method that enforces a global form of stability, which fails to identify the system, and a method that does not enforce any form of stability, which lacks theoretical guarantees. All proofs are omitted due to space limitations.

Notation: We define the sets of real and natural numbers as $\mathbb{R}$ and $\mathbb{N}$, respectively, with $\mathbb{N}_0 = \mathbb{N} \cup \{0\}$. For $x \in \mathbb{R}^n$, we define $|x|^2 \coloneqq x^\top x$ and $\|x\|_\infty = \sup_i |x^i|$, where x^i is the i-th element of x. We use $\star$ to denote symmetric terms in matrices. With $\mathbb{D}_+$, we denote the set of positive-definite diagonal matrices and $\mathbb{S}_+$ the set of positive-definite symmetric matrices. Given a positive-semidefinite matrix X, we define the ellipsoid $\mathcal{E}(X) \coloneqq \{x \in \mathbb{R}^n | x^\mathrm{T} X x \leq 1\}$. We consider sequences in the extended ℓ_{2e}^n space and define it as $\ell_{2e}^n \coloneqq \{(x_k)_{k\in\mathbb{N}_0} \mid x_k \in \mathbb{R}^n \text{ and } \sum_{k=0}^N |x_k|^2 < \infty \text{ for all } N \in \mathbb{N}_0\}$. Furthermore, for any real-valued matrix $H \in \mathbb{R}^{p\times n}$, we define the set $\mathcal{L}(H) \coloneqq \{x \in \mathbb{R}^n \,|\, \|Hx\|_\infty \leq 1\}$. We use $X \sim \mathcal{R}(a, b)$ to denote that the random variable X is drawn from a uniform distribution over the interval $(a, b) \subset \mathcal{R}$.

2. PROBLEM STATEMENT

We are given a set of M input-output trajectories from an unknown data-generating system, including an initial state x_0 defined as follows:

$$\mathcal{D} = \left\{ \left((y_k, u_k)_{k=0}^{N_i-1}, x_0 \right)^{[i]} \right\}_{i=1}^{M}, \tag{1}$$

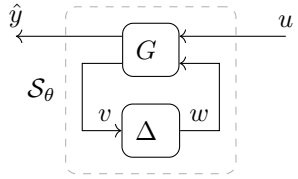

Fig. 1. Model (2) with static nonlinear function Δ.

where $\left((y_k, u_k)_{k=0}^{N_i-1}, x_0 \right)$ is a single trajectory of length N_i and $k \geq 0$ denotes the discrete time index. The trajectories u and y refer to the input and output respectively with $u_k \in \mathbb{R}^r$, $y_k \in \mathbb{R}^e$, and $x_0 \in \mathbb{R}^n$.

With the dataset $\mathcal{D}$, we aim to identify a nonlinear state space model $\mathcal{S}_\theta$ of the form

$$G \coloneqq \left\{ \begin{pmatrix} x_{k+1} \\ \hat{y}_k \\ v_k \end{pmatrix} = \begin{pmatrix} A & B & B_2 \\ C & D & D_{12} \\ C_2 & D_{21} & 0 \end{pmatrix} \begin{pmatrix} x_k \\ u_k \\ w_k \end{pmatrix} \right. \tag{2a}$$

with a static nonlinear function

$$w_k = \Delta(v_k), \tag{2b}$$

where $x_k \in \mathbb{R}^n$ refers to the internal state at discrete time step k. The external input and predicted output are denoted by $u_k \in \mathbb{R}^r$ and $\hat{y}_k \in \mathbb{R}^e$, respectively. The output $v_k \in \mathbb{R}^m$ is fed through the nonlinear function Δ and enters (2a) as $w_k \in \mathbb{R}^q$. The nonlinear activation function $\Delta : \mathbb{R}^m \to \mathbb{R}^q$ applies the same scalar function $\psi : \mathbb{R} \to \mathbb{R}$ elementwise; hence, $q = m$. A block diagram of model (2) is shown in Figure 1. The model parameters are collected in $\theta = \{A,\ B,\ B_2,\ C,\ D,\ D_{12},\ C_2,\ D_{21}\}$. The nonlinear state-space model (2) represents a wide class of networks; in particular, RNNs can be recovered by choosing $A = B = C = D = 0$, $B_2 = I$, and adding bias terms, as seen in, for example, in Goodfellow et al. (2016). Thus, we call model (2) a dynamic RNN.

In this work, we are interested in a regional form of stability. Hereto, we defined regional stability as follows.

Definition 1. (Regional stability). Consider the compact set $\mathcal{X} \subset \mathbb{R}^n$ and a set of admissible input trajectories $\mathcal{U} \subset \ell_{2e}^r$. The model $\mathcal{S}_\theta$ in (2) is regionally stable on $\mathcal{X}$ for $\mathcal{U}$ if for any $x_0 \in \mathcal{X}$ and input sequence from $\mathcal{U}$, the set $\mathcal{X}$ is forward invariant under the dynamics of $\mathcal{S}_\theta$.

The problem of identifying a model (2) that is regionally-stable given a data set (1) is formalized as follows.

Problem 2. Given a dataset $\mathcal{D}$ of the form (1), find the parameters θ of the model $\mathcal{S}_\theta$ in (2) such that $\mathcal{S}_\theta$ minimizes the MSE [1] between the predictions $\hat{y}$ and the outputs from the dataset y in $\mathcal{D}$ and is *regionally-stable* according to Definition 1 for some $\mathcal{X}$ and $\mathcal{U}$.

Note that the problem statement does not impose a predefined $\mathcal{X}$ and $\mathcal{U}$. Instead, these follow from the training procedure. In the next section, we will review the *standard* and *generalized* sector conditions before stating the main theoretical contribution of the paper, which is the key to solving Problem 2.

[1] We define the MSE as quadratic error between the predictions of model (2) and the outputs from the dataset (1), i.e., $\mathrm{MSE}(\hat{y}, y) \coloneqq \frac{1}{N} \sum_{k=0}^{N-1} |\hat{y}_k - y_k|^2$.

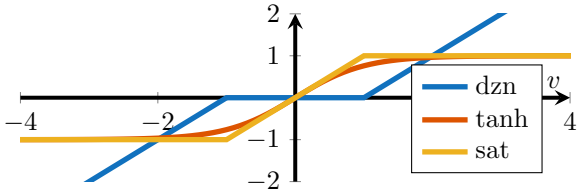

Fig. 2. Nonlinear activation functions.

3. REGIONAL STABILITY ANALYSIS FOR NONLINEAR SYSTEM IDENTIFICATION

The nonlinear model (2) is an interconnection between a linear model and a static, memoryless, and sector-bounded nonlinear function. In the literature, these models are known as *Lur'e*-type systems; see, for example, (Khalil, 2002; Shakib et al., 2022; Scherer, 2022). To assess their stability properties, sector conditions are used, as shown in Khalil (2002). First, we recall *standard* and *generalized* sector conditions, and then present convex constraints to guarantee regional stability of the learned model.

3.1 Sector-bounded nonlinearities

The scalar nonlinear function $\psi : \mathbb{R} \to \mathbb{R}$ in model (2) is said to satisfy *standard* sector conditions globally if the following inequality holds

$$\begin{pmatrix} \psi(v) \\ v \end{pmatrix}^{\mathrm{T}} \begin{pmatrix} -2 & 1 \\ 1 & 0 \end{pmatrix} \begin{pmatrix} \psi(v) \\ v \end{pmatrix} \geq 0 \tag{3}$$

for all $v \in \mathbb{R}$. The graph of functions that satisfy the *standard* sector condition lies in the sector defined by two lines with slopes 0 and 1. These bounds are conservative since they generally do not tightly cover the nonlinear shape of ψ. Therefore, global stability results that rely on standard sector conditions are often conservative too.

Lur'e-type systems, as in (2), are universal function approximators (Suykens et al., 1995). Changing the activation function from tanh, which is used in RNNs, to saturation (sat) does not affect this property. Moreover, applying a loop transformation (see Tarbouriech et al. (2006)), the saturation nonlinearity can be transformed to the deadzone nonlinearity $\psi : \mathbb{R} \mapsto \mathbb{R}$, defined by

$$\psi(v) \coloneqq \mathrm{dzn}(z) \coloneqq \begin{cases} 0 & \text{if } |v| \leq 1, \\ v - 1 & \text{if } v > 1, \\ v + 1 & \text{else } v > 1. \end{cases} \tag{4}$$

The graphs of the function tanh, sat, and dzn are displayed in Figure 2.

In model (2), we use the static decentralized deadzone nonlinear function (4) applied elementwise. Note that the resulting model is still a universal approximator; however, now we can use a state-dependent quadratic function

$$\Gamma(v, x, \Lambda, H) \coloneqq \begin{pmatrix} \Delta(v) \\ v + Hx \end{pmatrix}^{\mathrm{T}} \begin{pmatrix} -2\Lambda & \Lambda \\ \Lambda & 0 \end{pmatrix} \begin{pmatrix} \Delta(v) \\ v + Hx \end{pmatrix}, \tag{5}$$

which extends the *standard* sector condition by the following result.

Lemma 3. Consider the nonlinear operator $\Delta : \mathbb{R}^m \mapsto \mathbb{R}^q$ with activation function $\psi(z) = \mathrm{dzn}(z)$ applied elementwise, and matrices $\Lambda \in \mathbb{D}_+$ and $H \in \mathbb{R}^{m \times n}$. Then, for every $x \in \mathcal{L}(H)$ and $v \in \mathbb{R}^m$, we have

$$\Gamma(v, x, \Lambda, H) \geq 0. \tag{6}$$

We refer to (6) as the *generalized* sector conditions. Note that if H is zero, the *standard* sector conditions are recovered. However, if H is non-zero, then there is a region around x, namely $x \in \mathcal{L}(H)$, such that $\Gamma \geq 0$ holds.

Remark 4. The *generalized* sector conditions are studied in anti-wind-up controller design; see, for example, (Tarbouriech et al., 2006) and references therein.

3.2 Analysis result

We will now exploit the properties of *generalized* sector conditions to derive the sets $\mathcal{X}$ and $\mathcal{U}$ for regional stability. In controller design of neural network models, these properties have been used by La Bella et al. (2025) to ensure regional closed-loop stability. Therein, however, the closed-loop system is an autonomous system, i.e., the set $\mathcal{U}$ is the empty set, and $\mathcal{X}$ then is a region of attraction of the origin in Definition 1. For systems with inputs, the compact set $\mathcal{X}$ is no longer a region of attraction; instead, its forward invariance needs to be proven separately and depends on the set of admissible inputs $\mathcal{U}$.

In this work, we consider the following static set of inputs:

$$\mathcal{U}_\delta \coloneqq \left\{ (u_k \in \mathbb{R}^r)_{k \in \mathbb{N}} \mid u_k^{\mathrm{T}} u_k \leq \delta^2, \forall\, k \in \mathbb{N} \right\}, \tag{7}$$

which is defined through the constant $\delta \geq 0$. The following result provides sufficient conditions for regional stability. It characterizes the positively invariant set, i.e., the region $\mathcal{X}$ in the state space and the scalar δ.

Theorem 5. (Regional input-to-state stability). Given a discrete-time system (2) with parameters θ and decentralized deadzone nonlinearity $\Delta : \mathbb{R}^m \mapsto \mathbb{R}^q$, activation function $\psi(v) = \mathrm{dzn}(v)$ (4) applied elementwise, and consider a given scalar $\alpha \in (0, 1)$. Suppose there exist matrices $P \in \mathbb{S}_+$, $M \in \mathbb{D}_+$, $L = \begin{pmatrix} (l^1)^{\mathrm{T}} & \cdots & (l)^m)^{\mathrm{T}} \end{pmatrix}^{\mathrm{T}} \in \mathbb{R}^{m \times n}$, and scalar $s \in \mathbb{R}$ such that the LMIs

$$\underbrace{\left(\begin{array}{ccc|c} -\alpha^2 P & 0 & PC_2^{\mathrm{T}} + L^{\mathrm{T}} & PA^{\mathrm{T}} \\ \star & -I & D_{21}^{\mathrm{T}} & B^{\mathrm{T}} \\ \star & \star & -2M & MB_2^{\mathrm{T}} \\ \hline \star & \star & \star & -P \end{array}\right)}_{\mathbf{F}} \preceq 0,\ P \succ 0, \tag{8a}$$

and

$$\underbrace{\begin{pmatrix} 1/s^2 & l^i \\ (l^i)^{\mathrm{T}} & P \end{pmatrix}}_{\mathbf{G}_i} \succeq 0, \qquad \text{for all} \qquad i = 1, \ldots, m, \tag{8b}$$

are satisfied. Then, for any input sequence $u \in \mathcal{U}_\delta$ with

$$\delta^2 \leq (1 - \alpha^2) s^2, \tag{9}$$

the ellipsoid $\mathcal{E}(P^{-1}/s^2) \subset \mathcal{L}(H)$ is forward invariant with $H = LP^{-1}$. Moreover, for any $x_0 \in \mathcal{E}(P^{-1}/s^2)$ and input sequence $u \in \mathcal{U}_\delta$, the following bound is satisfied for any $k \geq 0$:

$$|x_k| \leq \min \left\{ \sqrt{\frac{\lambda_{\max}}{\lambda_{\min}}} \alpha^k |x_0| + \sqrt{\frac{1}{(1 - \alpha^2)\lambda_{\min}}} \sup_{0 \leq j < k} |u_k|, \; \frac{s}{\sqrt{\lambda_{\min}}} \right\}. \tag{10}$$

where $\lambda_{\min}$ and $\lambda_{\max}$ denote the minimum and maximum eigenvalues of the matrix P^{-1}.

Theorem 5 defines the size of input set $\mathcal{U}_\delta$ and the region $\mathcal{X} = \mathcal{E}(P^{-1}/s^2)$, required for regional stability in Definition 1. In addition, (10) characterizes the size of the state x_k, which depends on the size of the input. This is similar to a regional input-to-state stability result. In particular, for $u = 0$, the origin $x = 0$ is a locally exponentially stable equilibrium with the region of attraction $\mathcal{X}$. In the next section, the LMI constraints in Theorem 5 will be imposed during model training to ensure that the trained model is regionally stable.

Remark 6. Global stability is recovered for the case $H = 0$ ($L = 0$). In this case, we see from (9) that δ can be arbitrarily large since (8b) holds for any $s \geq 0$. The sets $\mathcal{X}$ is then the entire space $\mathbb{R}^{n\times n}$. Furthermore, then (3) implies a global input-to-state stability bound.

4. TRAINING

During training, we use the input-output dataset (1) to optimize the parameters θ of the system (2). In addition, the matrices P, M, and L, as well as the scalars s and α are optimized. Thus, the set of learnable parameters consists of $\omega = \{\theta,\ P,\ L,\ M,\ \alpha,\ s\}$. The objective of the optimization problem is to reduce the error between the prediction made by the model and the outputs in the training dataset

$$\begin{aligned} \min_{\omega} \quad & |\mathcal{S}_\theta(u, x_0) - y|^2 \\ \text{such that} \quad & (8) \text{ and } (9) \text{ hold, and } 0 < \alpha < 1. \end{aligned} \tag{11}$$

By the function $\mathcal{S}_\theta(u, x_0)$, we denote the predicted output response of model (2) for input u and initial condition x_0. Due to the recurrence of the model (2), the optimization problem (11) is nonlinear. The constraints, however, are affine with respect to the parameters P, L, M, s^2, which will be useful during initialization and training.

4.1 Interior-point method

We solve the optimization problem (11) iteratively using the Adam optimizer (Kingma and Ba, 2015), a stochastic gradient-descent method with momentum. To satisfy the conditions of (11), we utilize barrier functions, known from interior-point methods (see Boyd et al. (2004)). Intuitively, parameters close to the constraint boundary receive a large loss such that the resulting gradient does not point towards infeasible parameters. Given a constraint $\mathbf{C} \prec 0$, the associated barrier function is defined as

$$\phi(\mathbf{C}) := \begin{cases} -\log\det(-\mathbf{C}) & \text{if } \mathbf{C} \prec 0, \\ \infty & \text{if } \mathbf{C} \not\prec 0. \end{cases} \tag{12}$$

and it is added to the MSE between the prediction and the outputs from the training dataset. Thus, the training loss is defined as

$$\begin{aligned} \mathbf{L}(y, (u, x_0)) = & \frac{1}{N}|\mathcal{S}_\theta(u, x_0) - y|^2 + \\ & \nu\Big(\phi(\mathbf{F}) + \sum_{i=1}^{m} \phi(-\mathbf{G}_i) \\ & + \phi(\delta^2 - (1-\alpha^2)s^2) - \phi(1-\alpha) - \phi(\alpha)\Big). \end{aligned} \tag{13}$$

The matrices $\mathbf{F}$ and $\mathbf{G}_i$ stem from conditions (8) and the last line of (13) refers to the scalar inequality (9) and ensures that $\alpha \in (0,\ 1)$. The regularization parameter ν controls the influence of the barrier functions and can be scheduled during training.

The regularization is a soft constraint that does not guarantee that a new set of parameters satisfies the constraints (8) and (9). Therefore, after every epoch, we check these conditions using a Cholesky decomposition of the matrices $-\mathbf{F}$ and $\mathbf{G}_i$, and we verify scalar inequality (9) and the condition $\alpha \in (0, 1)$. In the case that the constraints are not satisfied after a parameter update, we fix the model parameters θ, s, α, and try to find P, L, M to satisfy conditions (8) and (9). This is a feasibility problem that can be formulated as an semidefinite program and solved efficiently with off-the-shelf solvers. If no feasible solution is found, the parameters are rolled back to the values before the update.

4.2 Initialization

To initialize the optimization problem, we aim to find a feasible initial model such that the barrier functions in the loss function (13) are bounded. The next proposition presents a method for finding such a feasible initial model.

Proposition 7. Take $\alpha = 0.99$, $A = 0.9I$, $C_2 = \mathcal{R}(-1, 1)$, $C = [I, 0]$, and $B_2 = D = D_{12} = 0$. Furthermore, given a user-specified $\delta > 0$, take $s = \sqrt{\frac{\delta^2}{(1-\alpha^2)}}$. If there exists parameters P, L, M, D_{21}, and B such that inequality (8) is satisfied, then model (2) satisfies all condition of Theorem 5. Furthermore, given a $\beta > 0$, if the LMI

$$\beta^2 I \preceq s^2 P \tag{14}$$

is satisfied, then any $x_0 \in \mathbb{R}^n$ that satisfies $|x_0|^2 \leq \beta^2$ is included in the set $\mathcal{E}(P^{-1}/s^2)$.

Proposition 7 ensures a feasible set of initial parameters, and thus the employed barrier functions are bounded. Furthermore, if additional information is available about the initial conditions that should be in the region $\mathcal{X}$, then the additional LMI constraint (14) can be used to ensure that a ball of radius β is contained in the region $\mathcal{X}$.

4.3 Post processing

After the training algorithm is finished, we analyze the learned model. We fix θ and α and optimize for a large compact set defined by $\mathcal{X}$ under the constraints given by the generalized sector conditions $\mathcal{E}(P^{-1}/s^2) \subset \mathcal{L}(H)$. This is achieved by minimizing $\hat{s} = 1/\sqrt{s}$ which appears in the following semidefinite program

$$\begin{aligned} \min_{\hat{s},P,L,M} \quad & \hat{s} \\ \text{such that} \quad & (8a),\ \begin{pmatrix} \hat{s} & l^i \\ (l^i)^\mathrm{T} & P \end{pmatrix} \succeq 0,\ i = 1, \dots m, \text{ and } (9). \end{aligned} \tag{15}$$

Then we get $s = \frac{1}{\sqrt{\hat{s}}}$, and $\mathcal{E}(P^{-1}/s^2) \subset \mathcal{L}(H)$.

5. NUMERICAL CASE STUDY

First, we introduce the unknown data-generating system and the baseline models. Then, we discuss the results and compare our method against two baselines.

5.1 Unknown data-generating system

To demonstrate the advantage of using generalized sector conditions in system identification with RNNs, we consider a synthetic nonlinear system with two states, i.e., $n = 2$, and a deadzone nonlinearity with $m = 2$. The state-space description in (2) is characterized by the matrices

$$\begin{pmatrix} A & B & B_2 \\ C & D & D_{12} \\ C_2 & D_{21} & 0 \end{pmatrix} = \begin{pmatrix} 0.998 & 0.096 & 0.0049 & 0.4191 & 0.4191 \\ -0.048 & 0.921 & 0.096 & 0.3744 & 0.3744 \\ 1 & 0 & 0 & 1 & 1 \\ 0.18 & 0 & 1 & 0 & 0 \\ 0 & 0.18 & 1 & 0 & 0 \end{pmatrix} \quad (16)$$

and deadzone nonlinear function $\psi = \mathrm{dzn}$. The system (16) satisfies all the conditions of Theorem 5 for a non-zero L and is regionally-stable according to Definition 1 (see Remark 6). The set of inputs is as in (7) with $\delta = \max_{k,i} |(u_k)^{[i]}|$ We used the system (16) to generate a dataset of the form (1). As inputs, we use

(i) $u = \sqrt{s^2(1-\alpha^2)}\sin(kdt)$
(ii) $u = \mathcal{R}(-\sqrt{s^2(1-\alpha^2)},\ \sqrt{s^2(1-\alpha^2)})$,

where s defines the size of the ellipsoidal region $\mathcal{X}$, $\alpha = 0.97$ is the contraction rate and $dt = 0.1$ refers to the sampling time. We used random initial conditions in the range $x_0^1, x_0^2 \in [-6,\ 6]$ and iterated the system for $N_i = N = 50$, steps for all i. We generated $M_{\sin} = 300$ samples with sinusoidal input (see (i)) and $M_{\text{noise}} = 300$ trajectories with noise input (see (ii)). In addition, we added $M_{\sin,\ \text{zero}} = M_{\text{noise},\ \text{zero}} = 150$ trajectories that start from $x_0 = [0,\ 0]^{\mathrm{T}}$. Thus, the input-output dataset consists of 45 000 datapoints and 900 trajectories. Note that some initial conditions are not in the set $\mathcal{X}$. Hence, some trajectories are in fact diverging.

We compare our model (GenSec (ours)) against a model that uses standard sector conditions (StdSec) and achieves global stability results in the form of input-to-state stability (see Remark 6), and against a model without constraints during learning (NoSec). The experiments in this work were conducted on an Intel i7 Laptop, and each model took approximately 50 minutes to train for 4000 epochs. The code can be found on GitHub [2] .

5.2 Discussion of results

In Figure 3(a), we see that the learned model GenSec (ours) is regionally stable, which is consistent with the data-generating system. Trajectories that diverge in the data-generating system also diverge for the learned model, and trajectories that end up in $\mathcal{X}$ also end up in the compact set. The model StdSec is globally input-to-state stable, as evidenced by the converging trajectories in Figure 3(b), even when the true system trajectories diverge, which is inconsistent. When we do not add any constraints (the model NoSec) on the learnable parameters, we have no stability guarantees and, consistent with the data-generating system, observe diverging trajectories, as shown in Figure 3(c). This underpins the theoretical results of Theorem 5, showing that with generalized sector conditions, we can recover the regional stability properties of the true system. With the proposed method, compared to global approaches, we extend the class of models that we can recover and achieve behavior that is consistent with the data-generating system.

[2] `https://github.com/Dany-L/genSecSysId`

Table 1. Evaluation results on test dataset for the different models.

Model	NRMSE	# params	m
NoSec	0.001581	24	2
StdSec	0.01635	33	2
GenSec (ours)	**0.0005698**	37	2

In Figure 4, this is shown in the time domain. The plot on the left shows a diverging trajectory. While GenSec (ours) and NoSec can recover such diverging behavior, the constraints in StdSec do not allow for regionally stable models. The model GenSec (ours) can recover converging and diverging trajectories from the training dataset, as shown in Figure 4. It also provides the compact set $\mathcal{X}$ and the input set $\mathcal{U}_\delta$ for reliable model use. The final loss values on the test dataset are shown in Table 1, and confirm that GenSec (ours) outperforms the baseline models in terms of prediction accuracy.

6. CONCLUSION

In this work, we have presented a method for learning regionally stable nonlinear models from input-output measurements. We presented convex constraints that enable analyzing the regional stability of dynamic RNNs. In addition, we proposed a learning algorithm that ensures these constraints are met during training by using barrier functions. Numerical experiments verify that the regionally stable models extend the class of learnable systems compared to globally stable dynamic RNNs.

The derived parametric constraints are conservative, and future work will address this. Furthermore, we aim to use our identification framework to learn dynamics from real-world datasets.

ACKNOWLEDGEMENTS

The author thanks Dr. Tobias Holicki, who gave the initial ideas and has helped to develop the analysis part.

DECLARATION OF GENERATIVE AI AND AI-ASSISTED TECHNOLOGIES IN THE WRITING PROCESS

During the preparation of this work, *Claude Sonnet 4.5 in Visual Studio Code* was used for coding assistance. After using this tool, the author(s) reviewed and edited the content as needed and takes full responsibility for the content of the publication.

REFERENCES

Beintema, G.I., Schoukens, M., and Tóth, R. (2023). Deep subspace encoders for nonlinear system identification. *Automatica*, 156, 111210.

Bonassi, F., Farina, M., Xie, J., and Scattolini, R. (2022). On recurrent neural networks for learning-based control: recent results and ideas for future developments. *Journal of Process Control*, 114, 92–104.

Boyd, S., Boyd, S.P., and Vandenberghe, L. (2004). *Convex optimization*. Cambridge university press.

Goodfellow, I., Bengio, Y., and Courville, A. (2016). *Deep learning*. MIT press.

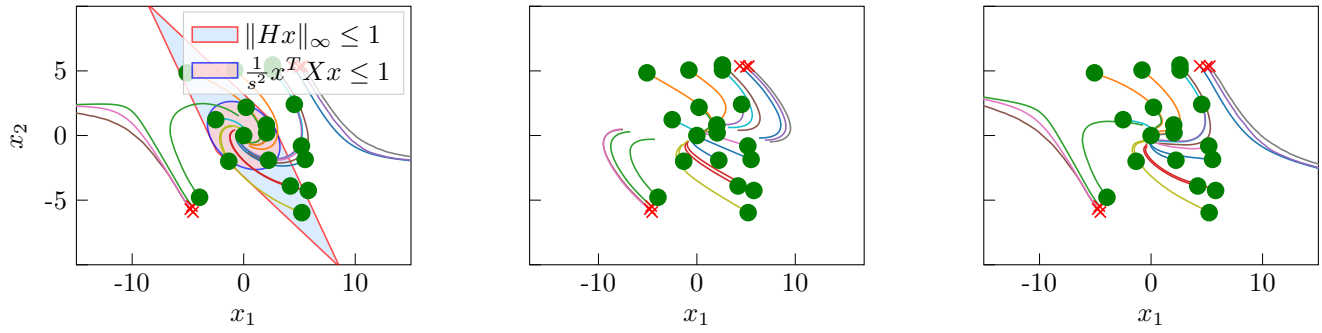

(a) GenSec (ours) (b) StdSec (c) NoSec

Fig. 3. Predictions made by the learned models in phase space, with excitation from the test dataset. The red crosses indicate initial conditions of trajectories that are diverging in the dataset, while the green dots indicate the ones that end up in $\mathcal{X}$. In (a), we see that the predictions made by our model are consistent with the dataset in the sense that when the trajectories from the dataset diverge, also the predicted trajectories diverge. In addition, we see the learned compact sets $\mathcal{E}(X/s^2)$ and $\mathcal{L}(H)$ in (a). The predictions of StdSec in (b) show that, even if the true system trajectories diverge, the models still predict converging responses, which is inconsistent and results from the imposed global stability conditions. The predictions of model NoSec in (c) are consistent but do not provide sets $\mathcal{X}$ or $\mathcal{U}_\delta$.

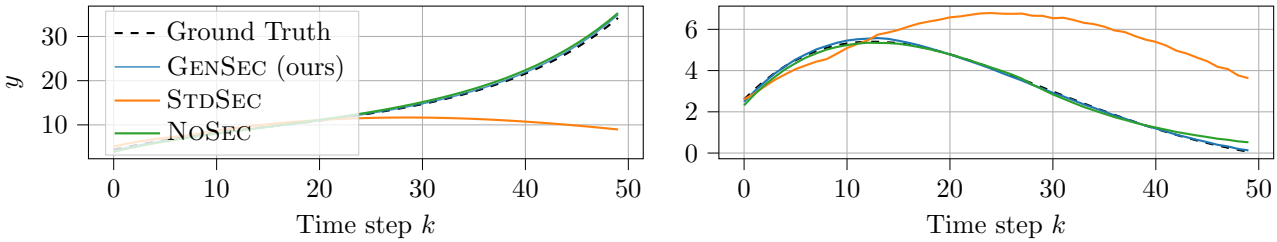

Fig. 4. Predictions of the models in the time domain compared to the outputs from the test dataset.

Khalil, H.K. (2002). *Nonlinear systems; 3rd ed.* Prentice-Hall, Upper Saddle River, NJ.

Kingma, D.P. and Ba, J. (2015). Adam: A method for stochastic optimization. In Y. Bengio and Y. LeCun (eds.), *3rd International Conference on Learning Representations, ICLR 2015, San Diego, CA, USA, May 7-9, 2015, Conference Track Proceedings*.

La Bella, A., Farina, M., D'Amico, W., and Zaccarian, L. (2025). Regional stability conditions for recurrent neural network-based control systems. *Automatica*, 174, 112127.

Ljung, L. (1999). *System Identification: Theory for the User*. Prentice Hall information and system sciences series. Prentice Hall PTR, second edition.

Mohajerin, N. and Waslander, S.L. (2019). Multistep prediction of dynamic systems with recurrent neural networks. *IEEE transactions on neural networks and learning systems*, 30(11), 3370–3383.

Pauli, P., Koch, A., Berberich, J., Kohler, P., and Allgöwer, F. (2021). Training robust neural networks using Lipschitz bounds. *IEEE Control Systems Letters*, 6, 121–126.

Revay, M., Wang, R., and Manchester, I.R. (2020). A convex parameterization of robust recurrent neural networks. *IEEE Control Systems Letters*, 5(4), 1363–1368.

Revay, M., Wang, R., and Manchester, I.R. (2023). Recurrent equilibrium networks: Flexible dynamic models with guaranteed stability and robustness. *IEEE Transactions on Automatic Control*, 69(5), 2855–2870.

Scherer, C.W. (2022). Dissipativity, convexity and tight O'Shea-Zames-Falb multipliers for safety guarantees. *IFAC-PapersOnLine*, 55(30), 150–155.

Shakib, M., Vervaet, N., Pogromsky, A., Pavlov, A., and van de Wouw, N. (2025). Numerical tools for the efficient steady-state optimization of discrete-time Lur'e-type control systems. *IFAC-PapersOnLine*, 59(19), 442–447. 13th IFAC Symposium on Nonlinear Control Systems NOLCOS 2025.

Shakib, M.F., Pogromsky, A.Y., Pavlov, A., and van de Wouw, N. (2022). Computationally efficient identification of continuous-time Lur'e-type systems with stability guarantees. *Automatica*, 136, 110012.

Shakib, M.F., Tóth, R., Pogromsky, A.Y., Pavlov, A., and van de Wouw, N. (2023). Kernel-based learning of stable nonlinear state-space models. In *2023 62nd IEEE Conference on Decision and Control (CDC)*, 2897–2902. IEEE.

Suykens, J.A., Vandewalle, J.P., and De Moor, B.L. (1995). *Artificial neural networks for modelling and control of non-linear systems*. Springer Science & Business Media.

Tarbouriech, S., Prieur, C., and da Silva, J.M.G. (2006). Stability analysis and stabilization of systems presenting nested saturations. *IEEE Transactions on Automatic Control*, 51(8), 1364–1371.

Yin, H., Seiler, P., and Arcak, M. (2021). Stability analysis using quadratic constraints for systems with neural network controllers. *IEEE Transactions on Automatic Control*, 67(4), 1980–1987.